IEEE Robotics and Automation Letters (RAL) paper presented at the
2020 IEEE/RSJ International Conference on Intelligent Robots and Systems (IROS)
October 25-29, 2020, Las Vegas, NV, USA (Virtual)

Fully Actuated Body-Mounted Robotic System for MRI-Guided Lower Back Pain Injections: Initial Phantom and Cadaver Studies*

Gang Li[1], Niravkumar A. Patel[1], Yanzhou Wang[1], Charles Dumoulin[2], Wolfgang Loew[2], Olivia Loparo[2], Katherine Schneider[2], Karun Sharma[3], Kevin Cleary[3], Jan Fritz[4], and Iulian Iordachita[1]

***Abstract*— This paper reports the improved design, system integration, and initial experimental evaluation of a fully actuated body-mounted robotic system for real-time MRI-guided lower back pain injections. The 6-DOF robot is composed of a 4-DOF needle alignment module and a 2-DOF remotely actuated needle driver module, which together provide a fully actuated manipulator that can operate inside the scanner bore during imaging. The system minimizes the need to move the patient in and out of the scanner during a procedure, and thus may shorten the procedure time and streamline the clinical workflow. The robot is devised with a compact and lightweight structure that can be attached directly to the patient's lower back via straps. This approach minimizes the effect of patient motion by allowing the robot to move with the patient. The robot is integrated with an image-based surgical planning module. A dedicated clinical workflow is proposed for robot-assisted lower back pain injections under real-time MRI guidance. Targeting accuracy of the system was evaluated with a real-time MRI-guided phantom study, demonstrating the mean absolute errors (MAE) of the tip position to be 1.50±0.68mm and of the needle angle to be 1.56±0.93°. An initial cadaver study was performed to validate the feasibility of the clinical workflow, indicating the maximum error of the position to be less than 1.90mm and of the angle to be less than 3.14°.**

Fig. 1: Experimental setup of the robotic system inside an MRI scanner. The 6-DOF robot was placed inside the scanner bore, and its 2-DOF needle driver was remotely actuated via a beaded chain transmission by the actuation box placed at the end of table. The radiologist can insert and rotate the needle remotely outside the scanner bore using the actuation box, while observing the real-time MR image feedback.

I. INTRODUCTION

Chronic lower back pain management is a significant clinical problem in both adult and pediatric patients. Approximately 80% of adults and 10% to 30% of young children experience lower back pain at some point in their lifetimes [1], [2]. Lumbar spinal injection is a common treatment for chronic lower back pain, which is commonly performed in the lower back and pelvis area, involving delivery of pain-relief medications to the facet joint, the narrow epidural space, the spinal nerve root, or the medial branches of dorsal rami [3]. Conventional lumbar spinal injections use X-ray, i.e. fluoroscopy or computed tomography (CT), to provide intervention guidance, which involves ionizing radiation exposure to both patients and physicians. Ultrasound is free of ionizing radiation, however, nerve visualization can be difficult, particularly for deep nerves such as those in obese patients and in the pelvis area. Conversely, magnetic resonance imaging (MRI) is an ideal imaging modality for lumbar spinal injections. MRI is able to provide unmatched soft tissue contrast and excellent anatomical details in real-time without exposing the patient or clinician to ionizing radiation, which is particularly critical for the reproductive organs in the lumbar spinal region and in pediatric patients [4]. However, the powerful magnetic field, strong radio frequency pulses, and narrow scanner bore present significant challenges to the development of robotic systems that can be compatible with the MRI environment.

To overcome these challenges, robotic systems have been investigated to operate within the MRI environment [5]. In terms of mounting mechanism, MRI-guided robots can be categorized as table-mounted and body-mounted systems. Table-mounted robots are usually mounted onto the scanner table and the patient is required to remain still throughout the procedure to maintain position with respect to the robot. Conversely, body-mounted robots are directly mounted to the patient using straps or other methods, attenuating effects of patient movement by moving with the patient. Table-mounted robots have been widely investigated for MRI-guided interventional procedures including stereotactic neurosurgery [6]–[8], prostate cancer therapy [9]–[12], liver ablation [13], and breast tissue biopsy [14]. Nevertheless, patient movement is unavoidable, particularly for procedures

*This work was funded by National Institutes of Health grant R01 EB025179

[1]Gang Li, Niravkumar A. Patel, Yanzhou Wang, and Iulian Iordachita are with Johns Hopkins University, Baltimore, MD, USA gli22@jhu.edu

[2]Charles Dumoulin, Wolfgang Loew, Olivia Loparo, and Katherine Schneider are with Cincinnati Childrens Hospital Medical Center, Cincinnati, OH, USA

[3]Karun Sharma and Kevin Cleary are with Childrens National Hospital, Washington, DC, USA

[4]Jan Fritz is with Johns Hopkins University School of Medicine, Baltimore, MD, USA

requiring a longer time. Consequently, mechanical fixtures, like the Leksell frame used in stereotactic neurosurgery [15], are typically utilized to prevent patient motion. By contrast, because dedicated supporting bases or frames are not required, body-mounted robots can be designed with compact and lightweight structures. Body-mounted robots have been developed for MRI-guided cryoablation [16], renal cancer interventions [17], abdominal interventions [18], and liver ablation [19]. Although these body-mounted robots have shown promise, they are not designed to provide six actuated degrees of freedom. Therefore, they may require the patient to be shuttled into the scanner bore for imaging and out for needle insertion during a procedure, which can be time-consuming. In addition, the "in and out" technique is incompatible with real-time monitoring, since the imaging and device insertion cannot be done at the same time. Hence, current body-mounted robots are not able to take advantage of real-time imaging for monitoring interventions, which is essential for real-time positioning feedback.

In our previous study, we reported the mechanical design of a 6-DOF fully actuated robotic assistant, performed kinematic analysis of the robot, evaluated its positioning accuracy in free space, and assessed its mounting stability [20]. In this study, we extend this work to improve the mechanical design and clinically integrate the system with real-time MRI guidance. The major contributions of this paper include: 1) improved design of the mounting mechanism that integrates a custom designed MRI coil and facilitates the attachment of the robot, 2) clinical integration of the system with image-based surgical planning, 3) creation of a dedicated clinical workflow for robot-assisted lower back pain injections under real-time MRI guidance, and 4) assessment of the system accuracy with an MRI-guided phantom study and validation of the clinical workflow with an initial cadaver torso study. In Section II, we describe the robotic system design, including the improved mechanical design and system integration. A dedicated clinical workflow for robot-assisted lower back pain injections is proposed in Section III. The experimental evaluation of the robotic system is presented in Section IV. Discussion about the results is reported in Section V. Conclusions are given in Section VI.

II. ROBOTIC SYSTEM DESIGN

A. Fully Actuated Robotic Manipulator

In this study, we improved the design of the mounting frame with a new sliding locking mechanism, and integrated a custom imaging coil to increase image quality. The CAD model of the improved robotic manipulator is illustrated in Fig. 2. The robot consists of a 4-DOF needle alignment module, a 2-DOF needle driver module, a fiducial frame, and a mounting frame. The 4-DOF needle alignment module is designed to align the needle to the desired pose with 2-DOF translational motion and 2-DOF rotational motion (see Fig. 2). Once the needle is aligned, the 4-DOF needle alignment module is turned off to reduce imaging noise. The 2-DOF needle driver module is designed to provide needle insertion and rotation (see Fig. 2), and is remotely actuated via a beaded chain transmission by an actuation box placed at the patient's feet. The 2-DOF needle driver can be operated in a manual or motorized mode through the remote actuation box. This feature provides enhanced safety in the event of motor failure and facilitates the user's learning curve since the clinicians can manipulate the needle manually as they do in current clinical practice. Note that, in this initial study, to be considered as a nonsignificant risk device [21], the needle driver was operated in the manual mode through the remote actuation box as described in Sec. IV. The detailed design of the actuation box was reported in [20], [22].

An earlier design of the locking mechanism using a flange slot mechanism to secure the robot was presented in our previous study [20]. The previous approach required the entire robot to be rotated to lock the mechanism, which is difficult when mounting the robot on the patient. A new locking mechanism was designed to secure the robot onto the mounting frame utilizing a sliding locking ring, as shown in Fig. 3. With this design, the mounting frame is first attached to the patient's lower back using straps. To attach the robot, the fiducial frame, which is fixed to the robot, is inserted into the slot on the mounting frame, and then the locking ring is rotated until it grips the fiducial frame. The new locking mechanism enables the robot to be attached more easily and with greater stability than the previous design.

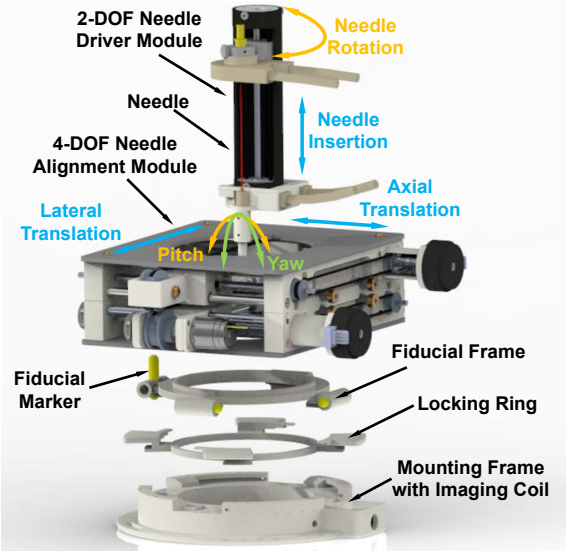

Fig. 2: CAD model of the 6-DOF body-mounted robot, demonstrating the major components, improved design of the mounting mechanism, integrated imaging coil, and degrees of freedom.

B. Embedded MR Imaging Coil

A new custom MR imaging coil is embedded in the mounting frame to provide enhanced imaging of patient anatomy and fiducial markers. An earlier design of the imaging coil which incorporated the coil into the base of the robot was presented in our previous study [23]. While the previous approach places the MR imaging coil close to the

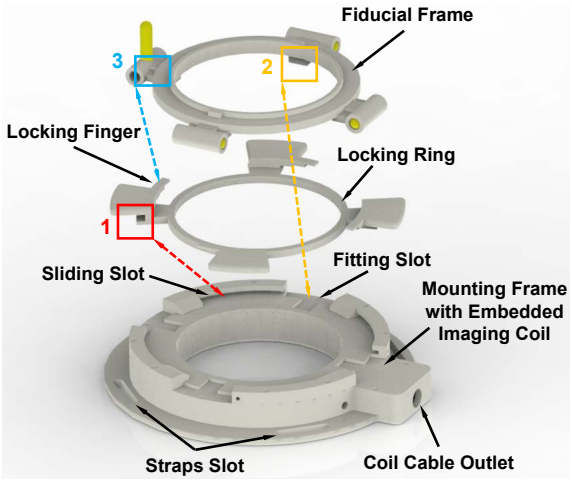

(a)

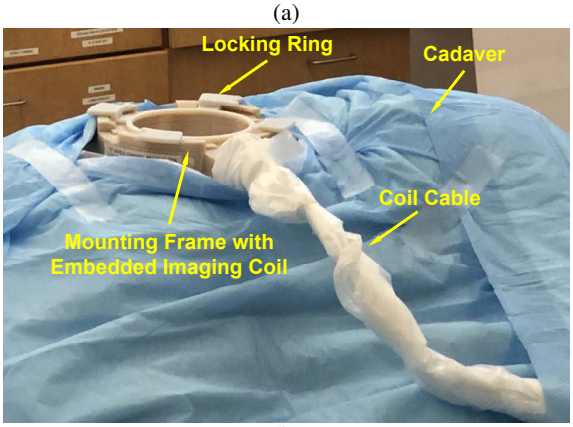

(b)

Fig. 3: Improved design of the mounting frame with embedded imaging coil. (a) Exploded CAD model of the mounting frame, showing the mating of components. The color numbers demonstrate the order to assemble the mounting frame. (b) Assembly of the mounting frame attached to the cadaver as presented in Sec. IV.

anatomy of interest and affords excellent imaging sensitivity, it has a major practical limitation. Since the tuning of the coil and placement of detuning diodes is scanner field and vendor specific, the direct incorporation of the coil into the robot limits the use of that robot to a specific MR scanner. To overcome this constraint the new coil was designed to be used independently of the robot, and act as a mounting base for the robot. The MR imaging coil incorporates straps that firmly attach it to the patient and a locking ring that allows the robot to be easily attached and detached as shown in Fig. 3. The base of the robot (which houses the fiducial markers) is keyed so that it only attaches to the MR imaging coil in one orientation. The sliding locking ring secures the robot so that the robot is rigidly connected to the coil, which in turn is firmly attached to the patient. This approach allows a single robot, or indeed a family of robots, to be used in a variety of MR scanners provided that each scanner has its own robot base imaging coil.

The MR imaging coil used in this study was a single loop coil similar to the coil used in our prior study [23], but was configured for use with our 1.5T Siemens Aera MRI scanner. The resonant frequency of the coil was tuned to match that of the MR scanner and the polarity of the active detuning diode was chosen to permit the scanner to dynamically detune the coil. The coil used distributed capacitance to minimize E-fields in the patient and a series of baluns to minimize common mode interactions with the robot cables and other conducting structures. The coil was attached to a single channel of an 8-channel preamplifier interface box (Stark Contrast MRI Coils Research, Erlangen, Germany), which has a connector that plugs into the Siemens scanner.

C. Robot Control System

The control system is composed of three main units as demonstrated in Fig. 4: 1) robot control software unit, 2) interface unit, and 3) controller unit. The robot control software includes a graphical user interface (GUI) based Matlab application (shown in Fig. 5), which manages the robot status, solves the robot kinematics, and generates high-level control commands, as well as communicates with the surgical planning platform as described in Sec. II-D. The interface unit contains the fiber optic media converter and power regulator. Optical fibers running through the wave guide connect the control PC and controller to prevent introduction of electromagnetic interference (EMI) into the scanner room. Regulated DC power is transmitted through a DB-9 connector on the shielded patch panel to reduce EMI. The controller unit is developed based on an 8-axis industrial-grade embedded controller (DMC 4183, Galil Motion Control, USA), providing high-precision closed-loop control of the robot with differential encoder based position feedback. Motion control commands generated from the Galil controller are sent to the PiezoMotor driver (PDA 3.1, PiezoMotor AB, Sweden) and Shinsei motor driver (D6060, Shinsei Corp., Japan) to drive the Piezo motors and Shinsei motors respectively. Power switches are installed on the motor drivers and used as a safety mechanism in case of control system failure. The controller unit is enclosed in an EMI shielded aluminum enclosure.

D. Surgical Planning

3D Slicer [24], an open source software platform, was adopted as the surgical planning workstation to visualize the intraoperative MR images, perform robot registration, and to plan and verify the needle path. As described in Sec. II-A, a fiducial frame was embedded in the robot for registration. At the beginning of each procedure, MR images of the fiducial markers are obtained and then segmented by the 3D Slicer software utilizing an embedded line marker registration (LMR) module [25] to register the robot to the MR image space. Once the robot is registered, the CAD model and a rendition of the robot's reachable workspace are overlaid onto the intraoperative MR images of the patient anatomy, providing guidance for the clinician, as demonstrated in Fig. 6. With this planning workstation, the clinician can define the desired needle path by selecting the target and entry points in the MR images. Once the needle is placed,

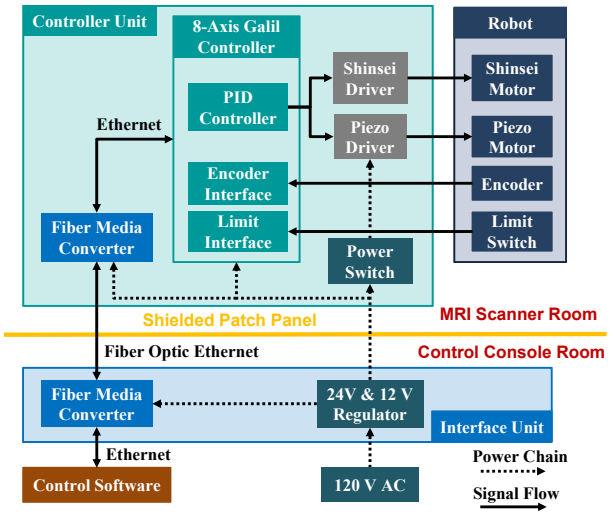

Fig. 4: Block diagram of the control system architecture, showing the controller unit inside the MRI scanner room providing closed-loop control of the robot and the interface unit inside the control console room containing the fiber optic media converter and power regulator.

confirmation images are acquired and the actual needle path can be visualized in 3D Slicer for verification.

III. CLINICAL WORKFLOW

Good clinical workflow design is critical for developing medical robotic systems, because the workflow provides requirements for the design of robotic systems and reflects the constraints of the clinical environment. The clinical workflow was developed through consultation with our clinical leads based on the conventional freehand MRI-guided procedures [26]. The proposed workflow consists of the following eight main steps, as illustrated in Fig. 7.

1) Position the patient on the MRI table outside the bore and create a sterile environment.
2) Initialize and secure the robot on the patient using straps.
3) Move the patient inside the scanner bore. Scan the anatomy of interest and register the robot with fiducial markers.
4) Plan the needle path on the planning workstation.
5) Align the needle with the robotic manipulator.
6) Insert the needle remotely with robotic assistance under real-time MRI guidance.
7) Inject medication under real-time MRI guidance and acquire high-resolution diagnostic images.
8) Retract the needle. Move the patient out of the scanner bore. Remove the robot and patient.

For conventional freehand MRI-guided procedures, the needle placement and verification steps typically require multiple attempts using an advance and check strategy. These steps take time, especially moving the patient in and out of the scanner bore and re-imaging with each needle advance, while the patient must remain still inside the scanner, thereby increasing patient discomfort (and anesthesia duration when

Fig. 5: Graphical user interface (GUI) of the robot control software executes five major functions: 1) communication with the embedded controller, 2) robot initialization, 3) individual axis control, 4) communication with the surgical planning workstation to acquire registration and planning information, and 5) needle driver control interface.

used). Such multi-step MRI-guided procedures increase the MRI room time and overall procedure cost and can also cause logistical problems in scanner usage and physician scheduling. By contrast, the proposed workflow, with robotic assistance, enables the intervention to be done all inside the scanner bore. Therefore, the real-time MRI-guided robotic system may provide significant benefits for lower back pain injections with a streamlined clinical workflow.

IV. EXPERIMENTS AND RESULTS

A. Experimental Setup

In our previous study [20], we evaluated the system positioning accuracy in free space and found the mean absolute error (MAE) of the needle tip position to be $0.99 \pm 0.46mm$ and of the insertion angle error to be $0.99 \pm 0.65°$. These results provided sufficient accuracy and repeatability of the mechanical system in free space, which met the design requirements presented in [20]. In this study, the system positioning accuracy was further evaluated with an MRI-guided phantom study and the proposed clinical workflow was validated with an initial cadaver torso study.

The phantom study was performed inside a 1.5T Siemens Aera scanner and included two tasks: the accuracy was

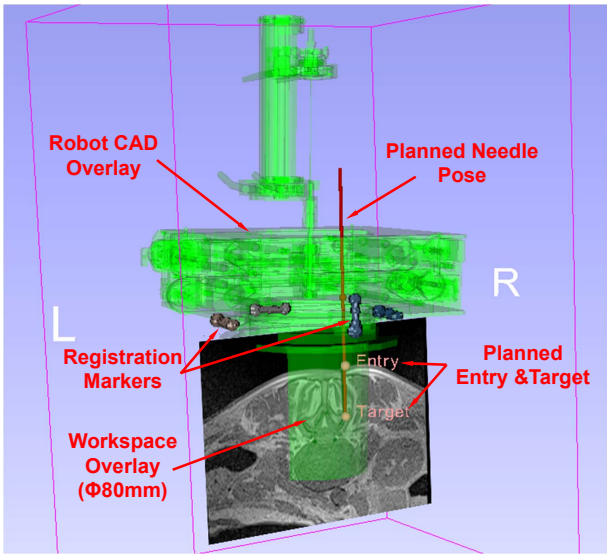

Fig. 6: Surgical planning platform, showing the CAD model and workspace of the robot overlaid on an intraoperative MR image, and the planned needle pose.

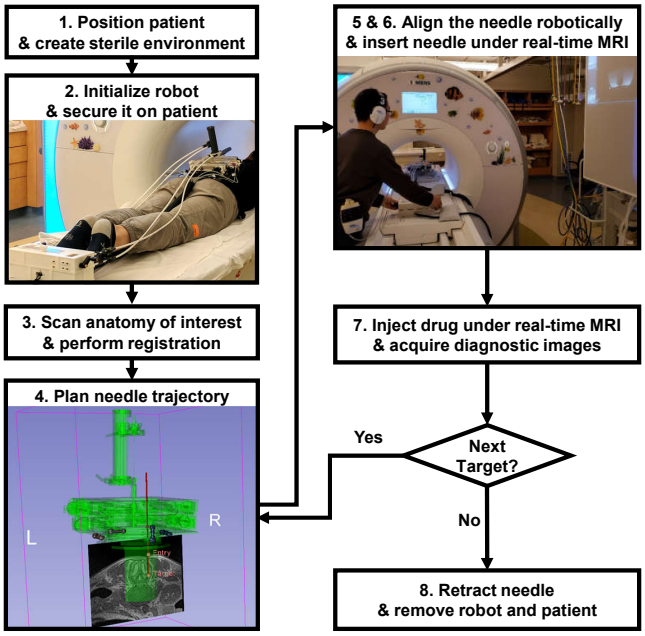

Fig. 7: Clinical workflow of robot-assisted lower back pain injections under real-time MRI-guidance.

first evaluated under static MRI guidance and second under real-time MRI guidance for comparison. Fig. 1 shows the experimental setup under real-time MRI guidance, and an equivalent setup was used for the study under static MRI guidance. The phantom was made of regular liquid plastic (Original Floating Plastic, M-F Manufacturing, USA), with an embedded plastic human lumbar spine model (XINDAM, Xindamai, China) as an anatomical target. A detailed explanation of the phantom was reported in [27]. A 20G MRI-compatible bevel-tipped needle (MReye, Cook Inc., USA) was utilized for the insertions.

A cadaver torso obtained from Science Care Inc. (Phoenix, Arizona) was used as the biological specimen and was placed in the prone position on the MRI table, as shown in Fig. 8. Permission was obtained from the hospital Office of Infection Control for this study. The robot was attached to the back of the cadaver using the mounting mechanism as described in Sec. II-A. The procedures were performed by an interventional radiologist and followed the clinical workflow proposed in Sec. III.

B. Positioning Accuracy Evaluation with MRI-Guided Phantom Study

For the first task, intraoperative MR images were obtained for planning the desired needle trajectories as described in Sec. II-D. Three targets were randomly selected on the lumbar spine phantom and the insertions were performed under the guidance of the same static MR images used for planning. Confirmation images, T2-weighted turbo spin echo (T2W-TSE) (TE: 32ms, TR: 2170ms, flip angle: 150°, slice thickness: 3mm, pixel spacing: 0.70mm x 0.70mm), were acquired after the insertions to measure the actual needle trajectories. The experiment results are summarized in Table. I, indicating the MAE of the target to be 2.31±0.73mm and of the angle to be 1.55±0.33°.

TABLE I: Experiment Results of Phantom Study under Static MRI Guidance

NO	Target (mm)			Entry (mm)			‖Error‖ (mm-deg)		
	R	A	S	R	A	S	Target	Entry	Angle
1	22.62	-83.17	-15.08	24.37	-41.93	-15.08	1.60	1.91	1.96
2	-5.73	-80.36	-17.89	-7.72	-41.94	-17.89	2.02	2.11	1.16
3	33.85	-94.68	-22.11	30.61	-45.00	-22.11	3.31	2.52	1.54
MAE							2.31	2.18	1.55
STD							0.73	0.25	0.33

TABLE II: Experiment Results of Phantom Study under Real-Time MRI Guidance

NO	Target (mm)			Entry (mm)			‖Error‖ (mm-deg)		
	R	A	S	R	A	S	Target	Entry	Angle
1	-28.93	-73.48	24.00	-34.29	-35.96	24.00	2.23	0.74	2.85
2	-14.40	-76.55	-4.14	-14.40	-39.77	-4.14	2.06	1.14	2.36
3	22.44	-75.32	-2.18	26.61	-40.90	-2.18	1.49	1.45	0.66
4	-10.95	-79.15	-13.30	-16.86	-42.29	-13.30	1.40	1.60	1.47
5	18.22	-78.04	-7.41	19.49	-42.32	-7.41	1.68	0.92	1.85
6	-21.34	-90.48	25.96	-18.62	-42.78	25.19	0.12	0.05	0.16
MAE							1.50	0.98	1.56
STD							0.68	0.51	0.93

For the second task, intraoperative MR images were taken for planning and the needle was placed under real-time MRI guidance (imaging frequency: 1.46Hz, TE: 1.67ms, TR: 189.94ms, flip angle: 45°, slice thickness: 5mm, pixel spacing: 2.0mm x 2.0mm). Once the needle was placed, confirmation images were acquired to measure the actual needle trajectories. The experiment results are summarized in Table. II, indicating the MAE of the target to be 1.50±0.68mm and of the angle to be 1.56±0.93°.

C. Initial Cadaver Study

Intermittent MR images were taken for every 2mm insertion advance to visualize needle position and progress towards the target. Real-time imaging was not used for this cadaver study, since we are still optimizing the imaging protocol to better visualize the anatomy and to reduce the needle artifact. Two target locations were defined within the facet joint and epidural space, as shown in Fig. 9, which are the typical region of lumbar spinal injections. During the insertions, the cadaver remained inside the scanner without being moved out, and the radiologist maneuvered the needle remotely through the needle driver actuation box outside the scanner. The positioning accuracy of the facet joint insertion gave a target error of 1.30mm and angular error of 0.87°. For the epidural space insertion the values were target error of 1.90mm and angular error of 3.14°.

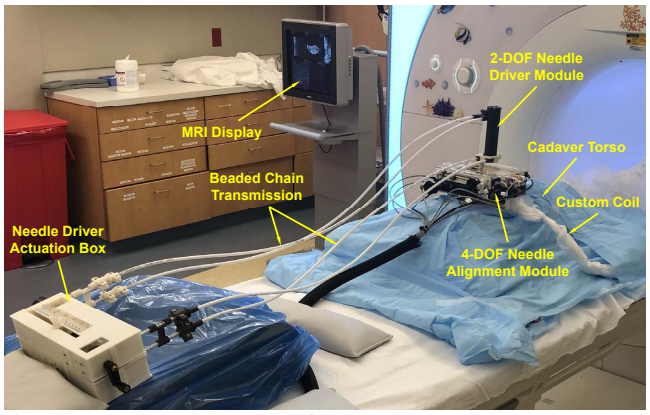

Fig. 8: Experimental setup of the cadaver torso study. The 6-DOF robot was attached to the lower back of torso via straps. The needle driver was remotely actuated by the actuation box via beaded chain transmission. The radiologist performed the intervention under the guidance of intermittent MR imaging control as shown on the display.

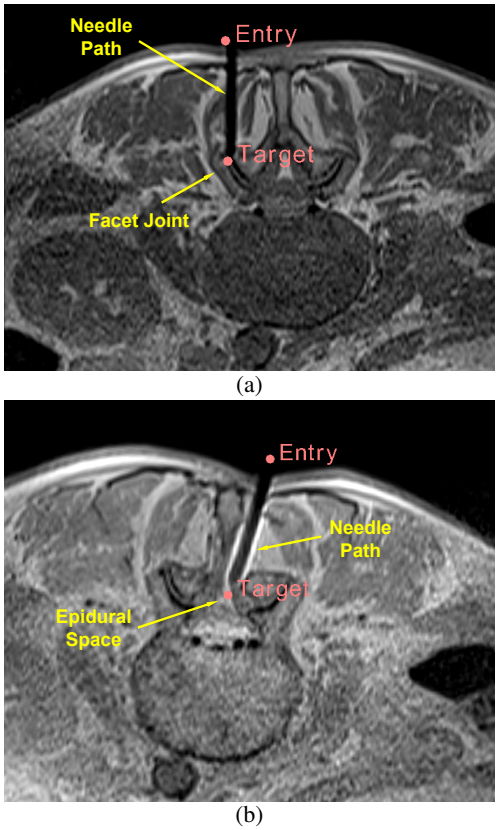

Fig. 9: MR images of two needles were placed within the facet joint (a) and epidural space (b) in the cadaver torso.

V. DISCUSSION

Comparing the results in Table. I and Table. II, it shows that real-time MRI-guided needle insertions have better accuracy with the MAE of the target reduced by 0.8mm, because the user can adjust the needle path on-line by steering the needle with real-time imaging feedback. While the fully actuated robotic assistant with remote actuation can eliminate the need to move the patient in and out of the scanner bore during the procedure, haptic feedback is minimal. Real-time imaging has the potential to address this gap and will be the subject of future work. The cadaver torso study verified the validity of the proposed clinical workflow. The spatial and orientation accuracy of the system are in accordance with a previously reported study on MRI-guided lumbar spinal injections with augmented reality visualization which demonstrated target error of 1.9±0.9mm [28]. The benefits of the remote actuation were confirmed by our clinical leads, including the improved ergonomics and streamlined workflow. Fig. 9 shows that the imaging signal of the lumbar spine is high and sufficient to visualize the anatomical structure with the imaging coil attached to the lower back. By contrast, in the conventional MRI-guided approach, the image can be relatively dark in the region of lumbar spine, especially when the patient is in the prone position. The use of an imaging coil at the base of the robot provides enhanced imaging quality for visualizing the patient anatomy.

In spite of the promising results of this study, there are some limitations. The statistical analysis was limited due to the limited number of initial trials. Further repeat trials are necessary to reach more definitive conclusions. The real-time imaging was not used for the cadaver study and will be implemented in a future study. This was an initial validation study and additional sterilization details still need to be addressed. The sterilization plan is to first drape the patient in the conventional manner and then make the needle guide stage sterilizable while draping the rest of the robot. In addition, the timing of the workflow was not measured. The size of the robot could also be further reduced to accommodate bigger patients. Because a phantom and a cadaver were used in this study, the patient motion (e.g. respiration and movement) was not taken into account, which may cause additional positioning error. However, based on our previous mounting stability study [20], we expect that the effect of patient motion would be minimal, and might be compensated by adjusting the needle path under real-time MRI guidance.

VI. CONCLUSIONS

This study reports the improved mechanism design, system integration, and initial phantom and cadaver studies of a fully actuated body-mounted robotic system for MRI-guided lower back pain injections. An improved mounting frame was designed to integrate a custom developed MRI coil and to facilitate the attachment of the robot to the patient. The system consists of a 6-DOF robot manipulator, a robot control module, and an image-based surgical planning workstation. A dedicated clinical workflow was proposed for robot-assisted MRI-guided lumbar spinal injections based on the freehand MRI-guided procedure. Initial phantom and cadaver studies were performed to assess the system positioning accuracy and to validate the proposed clinical workflow. Future work will focus on more compact mechanical design, a more thorough evaluation with additional cadaver tests, and a patient motion study.

ACKNOWLEDGMENT

The authors would like to thank Lu Vargas and Nicholas Mouzakis for helping with the MRI scanning, and thank Helmut Stark for providing the coil interface box.

REFERENCES

[1] "Low-back pain and complementary health approaches: What you need to know." https://www.nccih.nih.gov/health/low-back-pain-and-complementary-health/-approaches-what-you-need-to-know, Accessed April 30, 2020.

[2] F. Altaf and M. K. S. Heran, "Back pain in children and adolescents," *Bone Joint J*, vol. 96, no. 6, pp. 717–723, 2014.

[3] J. Fritz, T. Niemeyer, S. Clasen, J. Wiskirchen, G. Tepe, B. Kastler, T. Nagele, C. W. Konig, C. D. Claussen, and P. L. Pereira, "Management of chronic low back pain: rationales, principles, and targets of imaging-guided spinal injections," *Radiographics*, vol. 27, no. 6, pp. 1751–1771, 2007.

[4] K. A. Smith and J. Carrino, "Mri-guided interventions of the musculoskeletal system," *Journal of Magnetic Resonance Imaging: An Official Journal of the International Society for Magnetic Resonance in Medicine*, vol. 27, no. 2, pp. 339–346, 2008.

[5] R. Monfaredi, K. Cleary, and K. Sharma, "Mri robots for needle-based interventions: systems and technology," *Annals of biomedical engineering*, vol. 46, no. 10, pp. 1479–1497, 2018.

[6] G. Li, H. Su, G. Cole, W. Shang, K. Harrington, A. Camilo, J. G. Pilitsis, and G. S. Fischer, "Robotic System for MRI-Guided Stereotactic Neurosurgery," *Biomedical Engineering, IEEE Transactions on*, vol. 62, no. 4, pp. 1077–1088, 2015.

[7] Y. Kim, S. S. Cheng, M. Diakite, R. P. Gullapalli, J. M. Simard, and J. P. Desai, "Toward the development of a flexible mesoscale mri-compatible neurosurgical continuum robot," *IEEE Transactions on Robotics*, vol. 33, no. 6, pp. 1386–1397, 2017.

[8] S. Lwu and G. R. Sutherland, "The development of robotics for interventional mri," *Neurosurgery Clinics of North America*, vol. 20, no. 2, pp. 193–206, 2009.

[9] D. Stoianovici, C. Kim, D. Petrisor, C. Jun, S. Lim, M. W. Ball, A. Ross, K. J. Macura, and M. E. Allaf, "Mr safe robot, fda clearance, safety and feasibility of prostate biopsy clinical trial," *IEEE/ASME Transactions on Mechatronics*, vol. 22, no. 1, pp. 115–126, 2017.

[10] H. Su, W. Shang, G. Cole, G. Li, K. Harrington, A. Camilo, J. Tokuda, C. M. Tempany, N. Hata, and G. S. Fischer, "Piezoelectrically actuated robotic system for mri-guided prostate percutaneous therapy," *IEEE/ASME Transactions on Mechatronics*, vol. 20, no. 4, pp. 1920–1932, 2015.

[11] N. A. Patel, G. Li, W. Shang, M. Wartenberg, T. Heffter, E. C. Burdette, I. Iordachita, J. Tokuda, N. Hata, C. M. Tempany, *et al.*, "System integration and preliminary clinical evaluation of a robotic system for mri-guided transperineal prostate biopsy," *Journal of medical robotics research*, vol. 4, no. 02, p. 1950001, 2019.

[12] R. Seifabadi, M. Li, S. Xu, A. H. Negussie, Z. T. H. Tse, and B. J. Wood, "Mri robot for prostate focal laser ablation: a phantom study," in *Medical Imaging 2019: Image-Guided Procedures, Robotic Interventions, and Modeling*, vol. 10951, p. 109510N, International Society for Optics and Photonics, 2019.

[13] E. Franco, D. Brujic, M. Rea, W. M. Gedroyc, and M. Ristic, "Needle-guiding robot for laser ablation of liver tumors under mri guidance," *IEEE/ASME Transactions on Mechatronics*, vol. 21, no. 2, pp. 931–944, 2015.

[14] K. G. Chan, T. Fielding, and M. Anvari, "An image-guided automated robot for mri breast biopsy," *The International Journal of Medical Robotics and Computer Assisted Surgery*, vol. 12, no. 3, pp. 461–477, 2016.

[15] "Leksell stereotactic system." https://www.elekta.com/neurosurgery/leksell-stereotactic-system/, Accessed April 30, 2020.

[16] F. Y. Wu, M. Torabi, A. Yamada, A. Golden, G. S. Fischer, K. Tuncali, D. D. Frey, and C. Walsh, "An mri coil-mounted multi-probe robotic positioner for cryoablation," 2013.

[17] J. Tokuda, L. Chauvin, B. Ninni, T. Kato, F. King, K. Tuncali, and N. Hata, "Motion compensation for mri-compatible patient-mounted needle guide device: estimation of targeting accuracy in mri-guided kidney cryoablations," *Physics in Medicine & Biology*, vol. 63, no. 8, p. 085010, 2018.

[18] J. Ghelfi, A. Moreau-Gaudry, N. Hungr, C. Fouard, B. Véron, M. Medici, E. Chipon, P. Cinquin, and I. Bricault, "Evaluation of the needle positioning accuracy of a light puncture robot under mri guidance: results of a clinical trial on healthy volunteers," *Cardiovascular and interventional radiology*, vol. 41, no. 9, pp. 1428–1435, 2018.

[19] Z. He, Z. Dong, G. Fang, J. D.-L. Ho, C. L. Cheung, H.-C. Chang, C.-N. Chong, Y.-K. Chan, T.-M. Chan, and K.-W. Kwok, "Design of a percutaneous mri-guided needle robot with soft fluid-driven actuator," *IEEE Robotics and Automation Letters*, 2020.

[20] G. Li, N. Patel, W. Liu, D. Wu, K. Sharma, K. Cleary, J. Fritz, and I. Iordachita, "A fully actuated body-mounted robotic assistant for mri-guided low back pain injection," in *Robotics and Automation (ICRA), IEEE International Conference on*, pp. 1–7, IEEE, 2020 (Accepted).

[21] "FDA IDE approval process." https://www.fda.gov/medical-devices/investigational-device-exemption-ide/ide-approval-process#non_sig_risk, Accessed May 16, 2019.

[22] D. Wu, G. Li, N. Patel, J. Yan, R. Monfaredi, K. Cleary, and I. Iordachita, "Remotely actuated needle driving device for mri-guided percutaneous interventions," in *2019 International Symposium on Medical Robotics (ISMR)*, pp. 1–7, IEEE, 2019.

[23] R. Monfaredi, W. Loew, C. Ireland, V. Beskin, R. Pratt, R. Giaquinto, C. Dumoulin, P. Li, K. Cleary, and K. Sharma, "An integrated mr imaging coil and body-mounted robot for mr-guided pediatric arthrography: Snr and phantom study," in *Medical Imaging 2019: Image-Guided Procedures, Robotic Interventions, and Modeling*, vol. 10951, p. 1095117, International Society for Optics and Photonics, 2019.

[24] "3d slicer." https://www.slicer.org/, Accessed April 30, 2020.

[25] J. Tokuda, S. Song, K. Tuncali, C. Tempany, and N. Hata, "Configurable Automatic Detection and Registration of Fiducial Frames for Device-to-Image Registration in MRI-Guided Prostate Interventions," pp. 355–362, 2013.

[26] J. Fritz, A. L. Dellon, E. H. Williams, A. J. Belzberg, and J. A. Carrino, "3-tesla high-field magnetic resonance neurography for guiding nerve blocks and its role in pain management," *Magnetic Resonance Imaging Clinics*, vol. 23, no. 4, pp. 533–545, 2015.

[27] G. Li, N. A. Patel, J. Hagemeister, J. Yan, D. Wu, K. Sharma, K. Cleary, and I. Iordachita, "Body-mounted robotic assistant for mri-guided low back pain injection," *International Journal of Computer Assisted Radiology and Surgery*, pp. 1–11, 2019.

[28] J. Fritz, P. U-Thainual, T. Ungi, A. J. Flammang, N. B. Cho, G. Fichtinger, I. I. Iordachita, and J. A. Carrino, "Augmented reality visualization with image overlay for mri-guided intervention: accuracy for lumbar spinal procedures with a 1.5-t mri system," *American Journal of Roentgenology*, vol. 198, no. 3, pp. W266–W273, 2012.